Optica Applicata, Vol. XLIV, No. 3, 2014
DOI: 10.5277/oa140306

Optical generation of ultra-wideband signals with a reconfigurable spectral notch-band

PENG XIANG*, YINFANG CHEN, DALEI CHEN, JIYONG ZHAO

College of Communications Engineering, PLA University of Science and Technology, 210007, Nanjing, China

*Corresponding author: sunshinetim@126.com

A novel method for optical generation of ultra-wideband signals with a reconfigurable spectral notch-band is proposed. In the proposed system, ultra-wideband signals are generated in the optical domain and an optical tunable delay line is deployed to introduce a notch-band to the spectral profile of the generated ultra-wideband signals, which can effectively avoid the signal interference between ultra-wideband signals and pre-planned narrowband wireless signals used in wireless local area networks (WLAN). A theoretical model describing the proposed system is derived; the optical generation and fiber transmission of ultra-wideband signals with a reconfigurable notch-band are demonstrated via computer simulations.

Keywords: ultra-wideband (UWB), ultra-wideband over fiber, notch-band, interference avoidance.

1. Introduction

Ultra-wideband (UWB) has attracted a lot of attention due to its potential applications in a wide variety of fields such as high speed wireless communication systems, personal area networks, sensor networks and radar systems [1]. It is well-known that the UWB signals are regulated by the Federal Communications Commission (FCC) of the United States in the frequency range of 3.1–10.6 GHz band (*i.e.*, baseband) and 22–29 GHz band (*i.e.*, millimeter-wave band) for short range communications and vehicular radar respectively [2]. One of the key concerns in the application of UWB technology is the generation of UWB signals that satisfy the FCC specified spectral mask. In recent years, photonic generation of UWB signals has attracted extensive research interests due to the advantages offered by modern photonics such as low loss, high bandwidth and immunity to electromagnetic interference. More importantly, photonic generation of UWB signals can provide good compatibility with the UWB-over-fiber technology, which is widely regarded as a promising solution to enable UWB wireless reach extension [3].

In the past few years, optical generation of UWB signals, both in baseband and millimeter-wave band, has attracted great research interests [2–8]. And all of the exiting works demonstrated optical generation of UWB signals with spectral profile satisfying the FCC spectral mask. However the issue about interference avoidance between UWB signals and other pre-planned narrowband wireless signals has not been fully addressed in these works. UWB signals, especially in baseband (3.1–10.6 GHz), can unavoidably overlap with the pre-planned narrowband radio signals such as the very prevalent wireless fidelity (Wi-Fi) signals used in WLAN, which typically operates in the frequency band around 5 GHz [9]. In order to realize the interference avoidance between the UWB and Wi-Fi signals, electronic UWB filters and antennas with narrow notch-band around 5 GHz were designed and fabricated [10, 11]. However, these electronic components usually have a fixed notch-band and lack of tunability, which limits their usage in more complicated environment. In UWB over fiber systems, the interference avoidance issue is highly desirable to be addressed in the optical domain, to fully explore the advantages offered by modern photonics. Very recently, a band-notched UWB pulse generator has been proposed based on a nonlinear operated polarization-to-intensity converter [12]. Microwave photonic filtering and a notch-band were introduced in the generated UWB power spectra to realize the interference avoidance.

In this paper, a novel method to generate baseband UWB signals with a reconfigurable spectral notch-band in the optical domain is proposed. The proposed method can generate UWB signals with an expected spectral notch-band around 5 GHz, with its power spectrum matching with FCC spectral mask. And the notch-band can be flexibly turned in a wide frequency range. The proposed method is verified via both mathematical models and computer simulations.

2. Principle and theoretical analysis

Figure 1 shows the schematic diagram of the proposed system, which consists of a laser diode (LD), a polarization modulator (PolM), an optical bandpass filter (OBPF), a tun-

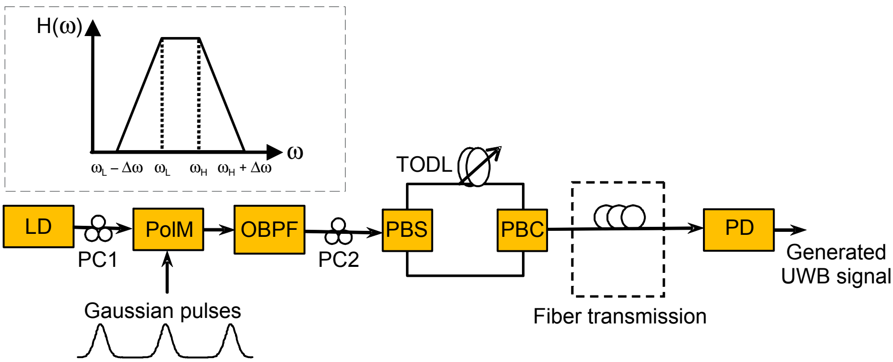

Fig. 1. Schematic diagram of the proposed UWB signal generation system. LD – laser diode, PolM – polarization modulator, OBPF – optical bandpass filter, PBS – polarization beam splitter, PBC – polarization beam combiner, PC – polarization controller, TODL – tunable optical delay line, PD – photodetector; insert – ideal response of an OBPF.

able optical delay line (TODL), two polarization controllers (PC), a polarization beam splitter (PBS) and a polarization beam combiner (PBC).

A light wave from the LD is sent to the PolM which is driven by an electronic Gaussian pulse source. The PolM is a special phase modulator that can support both TE (transverse electronic) and TM (transverse magnetic) modes with however opposite phase modulation indices [13].When a linearly polarized incident light is oriented with an angle of 45° to one principal axis of the PolM, complementary phase modulated optical fields at the output of the PolM along the two principal axes can be expressed as

$$\begin{bmatrix} E_x(t) \\ E_y(t) \end{bmatrix} = \exp(j\omega_c) \begin{bmatrix} \exp\left[j\beta\varphi(t)\right] \\ \exp\left[-j\beta\varphi(t)\right] \end{bmatrix} \tag{1}$$

where ω_c is the angular frequency of the optical carrier, β is the phase modulation index, and $\varphi(t)$ is the modulating (driving) signal.

The frequency response of an OBPF can be modeled as trapezium shape with two linear slopes, as shown in the insert of Fig. 1. Mathematically, its response can be written as [3]:

$$|H(\omega)| = \begin{cases} K\omega - K(\omega_L - \Delta\omega), & \omega_L - \Delta\omega \le \omega \le \omega_L \\ K\Delta\omega, & \omega_L \le \omega \le \omega_H \\ K(\omega_H + \Delta\omega) - K\omega, & \omega_H \le \omega \le \omega_H + \Delta\omega \end{cases} \tag{2}$$

where K is the slope of the filter ($K > 0$). If the phase modulated optical signal from PolM has a narrow bandwidth and the optical carrier is properly selected to be located at one of the linear slope, the impulse response of this OBPF can be approximated as:

$$h(t) = \begin{cases} -K(\omega_L - \Delta\omega)\delta(t) - jK\delta'(t), & \text{left slope} \\ K\Delta\omega\,\delta(t), & \text{center} \\ K(\omega_H + \Delta\omega)\delta(t) + jK\delta'(t), & \text{right slope} \end{cases} \tag{3}$$

where the group delay derived from the linear phase response is neglected, $\delta(t)$ is the unit impulse, and $\delta'(t)$ is the first-order derivative of the unit impulse. After the signals from PolM passing through the OBPF, the phase modulated optical signals along two polarization axes will be converted into intensity modulated optical signals. Assuming the optical signals are located at the left-slope of the OBPF, then the optical fields outputing from the OBPF can be expressed as:

$$\begin{bmatrix} e_{x1}(t) \\ e_{y1}(t) \end{bmatrix} = \begin{bmatrix} E_x(t) \\ E_y(t) \end{bmatrix} * h_{\text{left slope}}(t) \approx \begin{bmatrix} E_x(t)\left[K(\omega_c - \omega_L + \Delta\omega) + K\beta\varphi'(t)\right] \\ E_y(t)\left[K(\omega_c - \omega_L + \Delta\omega) - K\beta\varphi'(t)\right] \end{bmatrix} \tag{4}$$

where $*$ denotes the convolution operation, and $\varphi'(t)$ is the first-order derivative of the modulating signal $\varphi(t)$. It can be seen from Eq. (4), when $\varphi(t)$ is selected as Gaussian pulse, its first-order derivative, namely UWB monocycle shaped signals in the optical domain, can be acquired along both polarization axes.

Next, these two orthogonally polarized signal components are separated by a PBS and sent to its two outputs, with one component delayed by an TODL. Then they are combined by a PBC with their polarization state maintained, which can be written as

$$\begin{bmatrix} e_{x2}(t) \\ e_{y2}(t) \end{bmatrix} = \begin{bmatrix} e_{x1}(t) \\ e_{y1}(t-\tau) \end{bmatrix} \tag{5}$$

The signals are fed to a PD for optical-to-electrical conversion. Since these two signal components are orthogonally polarized, the problem associated with coherence interference in PD detection is avoided, and the photocurrent at the output of the PD can be written as

$$i_{\mathrm{PD}} = \left|e_{x2}(t)\right|^2 + \left|e_{y2}(t)\right|^2 \propto PK^2(\omega_c - \omega_L + \Delta\omega)\beta\left[\varphi'(t) - \varphi'(t-\tau)\right] \tag{6}$$

Note that in Eq. (6), the DC (direct current) and quadratic terms are neglected. The quadratic terms are usually very small compared with their linear counterpart under the assumption of small-signal modulation. And the DC component can be eliminated easily by a DC blocker. Therefore, the generated radio-frequency signals have a power spectral density (PSD) profile as follows:

$$S_{\mathrm{out}}(f) \propto \left|F\left[\varphi'(t)\right]\right|^2\left[1 - \cos(2\pi f\tau)\right] \tag{7}$$

where $F[\varphi'(t)]$ is the Fourier transform of $\varphi'(t)$, and has a spectral shape of monocycle signals, as inferred from Eq. (4). As can be seen from Eq. (7), the system output RF signals show a PSD profile of UWB monocycle signals multiplied by a cosine-based function. Since a cosine function is periodic, notch-bands are introduced to the signal spectrum, with a frequency spacing determined by $\Delta f_{\mathrm{notch}} = 1/\tau$, which can be easily reconfigured by turning the TODL. It is very straightforward to choose the notch-band at $f_{\mathrm{notch}} = 1/\tau$ to be the expected spectral notch for the generated UWB signals.

3. Simulation results and discussions

Figure 2 shows the simulation model of the proposed optical UWB signal generation system using a commercial software package Virtual Photonic Incorporation (VPI) Transmission maker. The simulation model is based on the schematic diagram in Fig. 1, where the light wave from the LD is sent to the PolM with its polarization state oriented with an angle of 45° to one principal axis of the PolM. Its center wavelength is adjusted to match the left slope of the OBPF frequency response. An electronic pulse

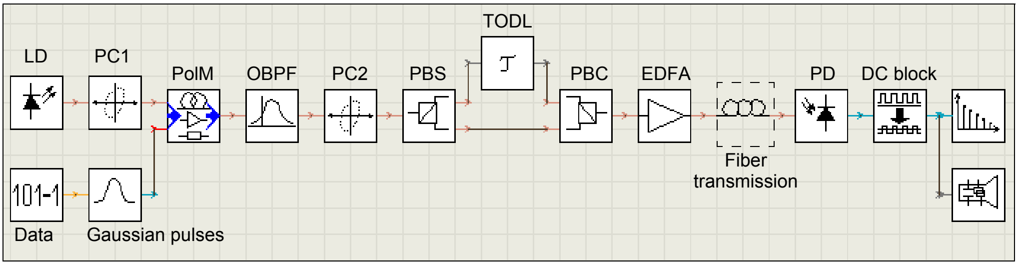

Fig. 2. Simulation model of the proposed system.

source which generates Gaussian pulses with a full-width at half-maximum (FWHM) pulsewidth of 60 ps is used to drive the PolM.

Firstly, optical generation of UWB signals with a notch-band located at 5 GHz is demonstrated by the simulation, where the TODL induced delay is set as $\tau = 200$ ps. Figure 3 shows the generated UWB signals and their power spectrum. The power spectrum peak is controlled to be –41.3 dBm by properly adjusting the LD output power, and compared with the FCC spectral mask.

As can be seen from Fig. 3**a**, the power spectrum of the generated UWB signal has an obvious notch-band at 5 GHz, and can fit into the FCC mask well. The notch-band

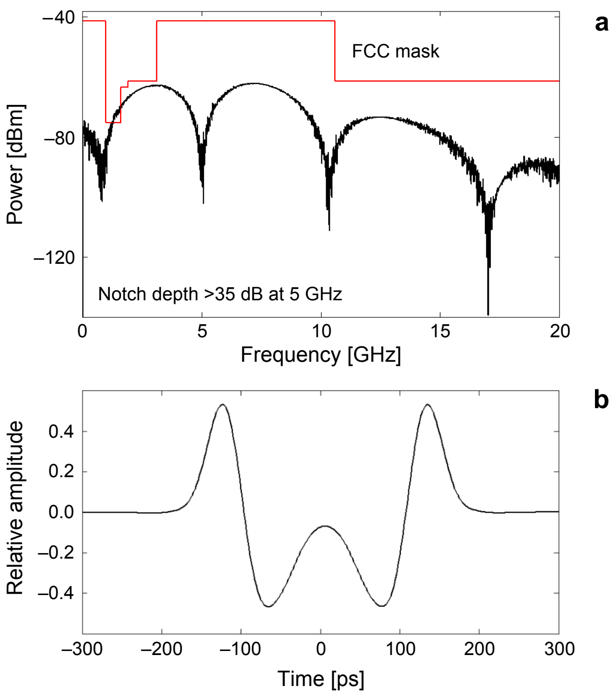

Fig. 3. The generated UWB signals with a spectral notch-band at 5GHz. Signal power spectrum (**a**), and UWB signal waveform (**b**).

depth reaches more than 35 dB calculated from the spectral peak, which can significantly reduce the signal interference between UWB and Wi-Fi signals. As seen from Fig. 3**b**, the generated UWB signal is composed of two polarity reversed monocycles, which can be explained by Eq. (6).

Secondly, the tunability of the notch-band in the generated UWB signal spectrum is demonstrated, where 5 frequency locations are chosen, namely: 4.5, 5.15, 5.8, 6.5, and 8 GHz. Accordingly, in these cases the time delay is set as 222, 194, 172, 154 and 125 ps, respectively. The simulation results are shown in Fig. 4.

As can be seen from Fig. 4**a**, the tuning of the expected notch-band in the generated UWB signal spectrum is successfully realized. Therefore the interference between UWB signals and other narrowband signals, including WLAN signals located at 5.1–5.8 GHz [10], can be avoided in a flexible manner.

In practical systems, the frequency tuning range and the precision of the spectral notch-band are determined by the time delay tuning range and the step size of the deployed TODL. Since TODL with a tuning range of 0–600 ps and a step size of less than 1 ps is commercially available, accurate frequency tuning of the expected notch-band within the total frequency band of UWB signals (namely 3.1–10.6 GHz) can be realized.

It is also noticed from Fig. 4**a** that when the expected notch-band is set at 4.5 GHz (τ = 222 ps), a second notch-band around 9 GHz will also be induced in the UWB power spectrum due to the periodicity of the notches as indicated in Eq. (7). Indeed, multiple notch-bands can be possibly introduced to UWB power spectrum when the time delay is set as $\tau > 200$ ps. However this may lead to unwanted notch-bands.

Figure 4**b** shows the corresponding UWB signal waveform when the time delay τ is set as 222, 194, 172, 154 and 125 ps, respectively. As can be seen, the generated UWB signal waveforms have longer time duration when τ is larger. The time duration of the generated UWB signals increases from 490 to 586 ps, as is increased from 125 to 222 ps.

For a practical UWB over fiber system, the generated UWB signals are usually required to be coded and transmitted over a distance of an optical fiber link [14]. In the third simulation scenario, the generated UWB signals are on-off-keying (OOK) coded by coding the electronic Gaussian pulse source, and transmitted over a span of an fiber-optic link. The transmission fiber is a span of polarization maintain fiber, which can be inserted before the PD in the system as indicated in the dashed box shown in Figs. 1 and 2. The simulation results are shown in Fig. 5, where the fiber link length is set as 0, 10 and 30 km. Signal bit rate is set as 1 Gbps, and pseudorandom binary sequence (PRBS) bit pattern is used. The signal spectral notch-band is chosen as f_{notch} = 5 GHz to avoid interference with Wi-Fi signals, and an erbium-doped fiber amplifier (EDFA) is deployed to compensate the fiber transmission loss.

As seen from Fig. 5**a**, the expected notch-band at 5 GHz remains after signal coding and fiber transmission. Discrete spectral lines with a frequency spacing of 1 GHz appear on the UWB signal power spectrum, which is corresponding to the bit rate of

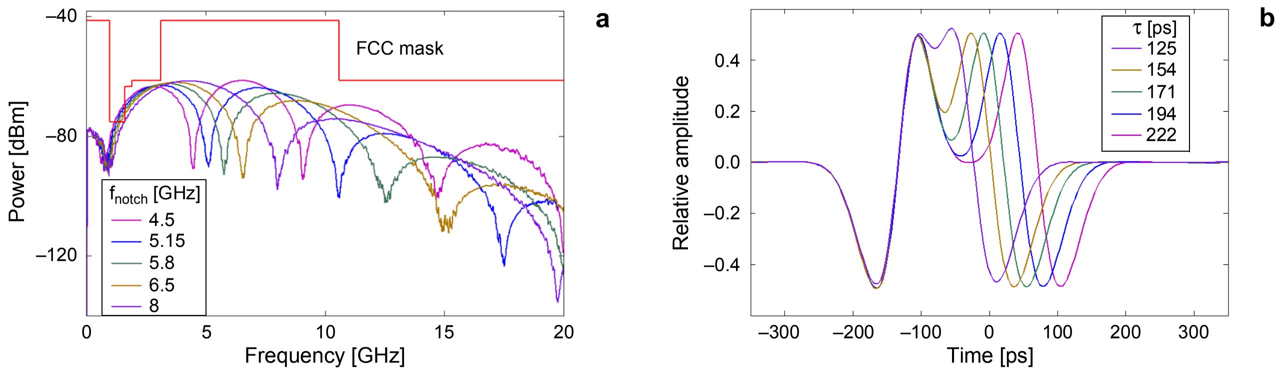

Fig. 4. Frequency tuning of expected spectral notch-band of UWB signals. Signal power spectrum (**a**), and UWB signal waveform (**b**).

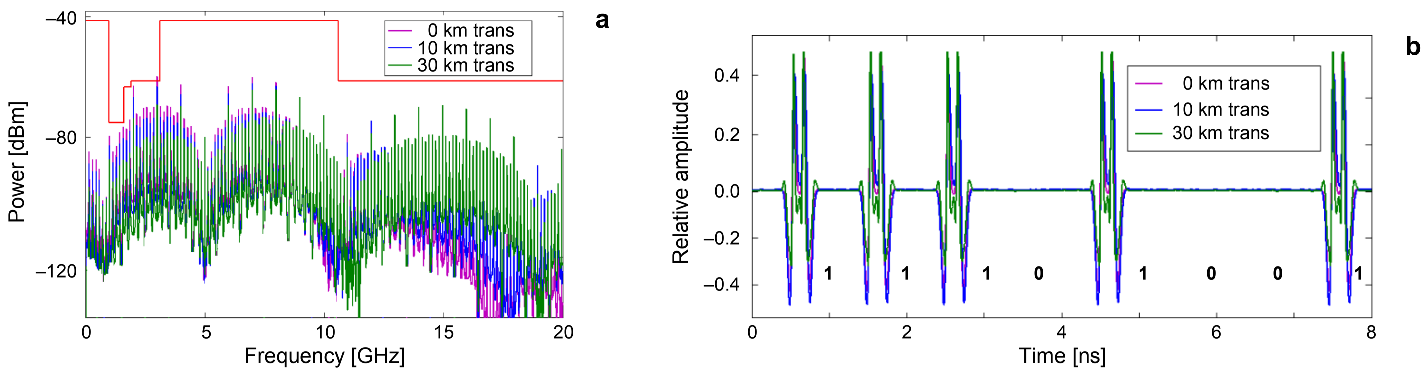

Fig. 5. The OOK coded UWB signals after 0, 10 and 30 km fiber transmission (trans). Signal power spectrum (**a**), and UWB signal waveform (**b**).

1 Gbps. These spectral lines can interfere with the notch-band of UWB spectrum if one of them happens to reach the notch-band frequency. This may weaken the interference avoidance function of the expected notch-band at 5 GHz. This problem can be easily eliminated by properly choosing the system bit rate, such as 2 Gbps [15], 781 Mbps [16], *etc.*, so that the spectral lines never overlap with the spectral notch-band.

As seen from Fig. 5**b**, the generated UWB signals suffer some minor distortions due to the fiber dispersion. Proper dispersion compensation techniques can be used to solve this problem. However, as indicated by the simulation results, when the fiber transmission distance is not very long (such as less than 10 km, typically the case for indoor application [2]), dispersion compensation may not be necessary.

In the proposed system, the coding processes are relatively independent of the UWB signal generation, so other coding schemes such as pulse-amplitude-modulation (PAM) and pulse-position-modulation (PPM) can also be easily implemented by properly coding the Gaussian pulse source.

4. Conclusion

A novel method for the generation of UWB signals with a reconfigurable notch-band in the optical domain is proposed and simulatively demonstrated. The notch-band can be widely tuned within the UWB spectrum by properly adjusting the TODL in the system, which can effectively realize the interference avoidance between UWB signals and existing narrowband radio signals, such as Wi-Fi signals used in WLAN systems. The proposed system can effectively exploit the benefits offered by modern photonics, and has great potential for application in UWB over fiber systems.

Acknowledgements – This work is supported by Jiangsu Province Natural Science Foundation under grant BK20140069 and National Nature Science Foundation of China (NSFC) under grant No. 61032005.

References

[1] PORCINO D., HIRT W., *Ultra-wideband radio technology: potential and challenges ahead*, IEEE Communications Magazine **41**(7), 2003, pp. 66–74.

[2] WEI LI, WEN TING WANG, WEN HUI SUN, JIAN GUO LIU, NING HUA ZHU, *Generation of FCC-compliant and background-free millimeter-wave ultrawideband signal based on nonlinear polarization rotation in a highly nonlinear fiber*, Optics Express **22**(9), 2014, pp. 10351–10358.

[3] JIANPING YAO, FEI ZENG, QING WANG, *Photonic generation of ultrawideband signals*, Journal of Lightwave Technology **25**(11), 2007, pp. 3219–3235.

[4] WEI LI, WEN TING WANG,WEN HUI SUN, LI XIAN WANG, NING HUA ZHU, *Photonic generation of background-free millimeter-wave ultra-wideband pulses based on a single dual-drive Mach–Zehnder modulator*, Optics Letters **39**(5), 2014, pp. 1201–1203.

[5] MING-JIANG ZHANG, TIE-GEN LIU, AN-BANG WANG, JIAN-YU ZHENG, LI-NA MENG, ZHAO-XIA ZHANG, YUN-CAI WANG, *Photonic ultrawideband signal generator using an optically injected chaotic semiconductor laser*, Optics Letters **36**(6), 2011, pp. 1008–1010.

[6] YUAN YU, JIANJI DONG, XIANG LI, XINLIANG ZHANG, *Ultra-wideband generation based on cascaded Mach–Zehnder modulators*, IEEE Photonics Technology Letters **23**(23), 2011, pp. 1754–1756.

[7] YANG YUE, HAO HUANG, LIN ZHANG, JIAN WANG, JENG-YUAN YANG, YILMAZ O.F., LEVY J.S., LIPSON M., WILLNER A.E., *UWB monocycle pulse generation using two-photon absorption in a silicon waveguide*, Optics Letters **37**(4), 2012, pp. 551–553.

[8] PENG XIANG, XIAOPING ZHENG, HANYI ZHANG, YUQUAN LI, JINTIAN XIONG, *A novel approach to all-optical generation of ultra-wideband signals*, Fiber and Integrated Optics **32**(3), 2013, pp. 222–232.

[9] YOUNG JUN CHO, KI HAK KIM, DONG HYUK CHOI, SEUNG SIK LEE, SEONG-OOK PARK, *A miniature UWB planar monopole antenna with 5-GHz band-rejection filter and the time-domain characteristics*, IEEE Transactions on Antennas and Propagation **54**(5), 2006, pp. 1453–1460.

[10] BAHADORI K., RAHMAT-SAMII Y., *A miniaturized elliptic-card UWB antenna with WLAN band rejection for wireless communications*, IEEE Transactions on Antennas and Propagation **55**(11), 2007, pp. 3326–3332.

[11] MONDAL P., YONG LIANG GUA, *A coplanar stripline ultra-wideband bandpass filter with notch band*, IEEE Microwave and Wireless Components Letters **20**(1),2010, pp. 22–24.

[12] JIANYU ZHENG, NINGHUA ZHU, HUI WANG, YUANXIN DU, LIXIAN WANG, JIANGUO LIU, *Photonic-assisted ultrawideband pulse generator with tunable notch filtering based on polarization-to-intensity conversion*, IEEE Photonics Journal **5**(3), 2013, article 7900909.

[13] SHILONG PAN, JIANPING YAO, *Performance evaluation of UWB signal transmission over optical fiber*, IEEE Journal on Selected Areas in Communications **28**(6), 2010, pp. 889–900.

[14] SHILONG PAN, JIANPING YAO, *UWB-over-fiber communications: modulation and transmission*, Journal of Lightwave Technology **28**(16), 2010, pp. 2445–2455.

[15] ADRAHA S.T., OKONKWO C.M., KOONEN A.M., TANGDIONGGA E., *Experimental demonstration of 2 Gbps IR-UWB over fiber using a novel pulse generation technique*, Presented at the Conference on Access Network and In-house Communications 2010, Karlsruhe, Germany, June 21–24, 2010, paper AthA5.

[16] XIANBIN YU, GIBBON T.B., MONROY I.T., *Experimental demonstration of all-optical 781.25-Mb/s binary phase-coded UWB signal generation and transmission*, IEEE Photonics Technology Letters **21**(17), 2009, pp. 1235–1237.

Received May 3, 2014
in revised form July 17, 2014